European Journal of Radiology Open 9 (2022) 100422

Contents lists available at ScienceDirect

European Journal of Radiology Open

journal homepage: www.elsevier.com/locate/ejro

Radiologic screening and surveillance in hereditary cancers

Jamie E. Clarke [a,b,1], Stephanie Magoon [a,1], Irman Forghani [c], Francesco Alessandrino [b], Gina D'Amato [d], Emily Jonczak [d], Ty K. Subhawong [b,*]

[a] Leonard M. Miller School of Medicine, University of Miami, Miami, Florida, USA
[b] Department of Radiology, Sylvester Comprehensive Cancer Center and the University of Miami Miller School of Medicine/Jackson Memorial Hospital, Miami, FL 33136, USA
[c] Department of Human Genetics, Miller School of Medicine, Miami, FL 33136, USA
[d] Department of Hematology/Oncology, Sylvester Comprehensive Cancer Center and the University of Miami Miller School of Medicine/Jackson Memorial Hospital, Miami, FL 33136, USA

HIGHLIGHTS

- Pathogenic germline mutations in hereditary cancers cause early-onset distinctive tumors in an organ-specific pattern.
- Geneticist, oncologist, and radiologist coordination facilitates syndrome-appropriate screening and surveillance strategies.
- WB-MRI is a promising comprehensive non-ionizing screening/surveillance modality but with sparse prospective survival data.

ARTICLE INFO

Keywords:
Radiology
Hereditary cancers
Screening
Surveillance
MRI
Whole-body MRI
PET/CT

ABSTRACT

Hereditary cancer syndromes comprise an important subset of cancers caused by pathogenic germline mutations that can affect various organ systems. Radiologic screening and surveillance for solid tumors has emerged as a critical component of patient management in permitting early cancer detection. Although imaging surveillance may be tailored for organ-specific cancer risks, surveillance protocols frequently utilize whole-body MRI or PET/CT because of their ability to identify neoplasms in different anatomic regions in a single exam. In this review, we discuss the basic tenets of imaging screening and surveillance strategies in these syndromes, highlighting the more common neoplasms and their associated multimodality imaging findings.

1. Introduction

Hereditary cancer syndromes are characterized by pathogenic germline mutations that lead to the early development of common or unique tumors in specific organs (Table 1). Most of these syndromes have an autosomal dominant inheritance pattern and account for 5–10% of all cancers (Tiwari et al., 2019). The key findings in hereditary cancer syndromes are early onset of cancers, bilateral tumors in paired organs or multiple organ involvement, as well as specific cancer patterns in a family or multiple family members affected with primary cancers. Establishing the diagnosis of a genetic syndrome directs appropriate screening and surveillance strategies for the affected individuals, and may prompt detection of additional at-risk family members[1]. Early identification of hereditary cancer syndromes and implementation of proper surveillance has improved life expectancy in hereditary cancer syndromes [2–4]. This has brought imaging into a central role in screening of these patients. In this article, we review the organ-specific pattern and distinctive tumor types that characterize some of these syndromes, emphasizing the role of imaging screening and surveillance.

2. PET/CT and whole body-MRI

Whole body PET/CT offers a combination of anatomic and functional imaging, and can be performed with a variety of radiotracers. Those most commonly used in hereditary cancer syndromes include conventional ^{18}F-fluorodeoxyglucose (^{18}F-FDG) to map areas of heightened glucose metabolism, and ^{68}Ga-DOTATATE to delineate neuroendocrine tumors expressing somatostatin receptors [5]. ^{18}F-FDG is an analog of

* Correspondence to: Department of Radiology, 1611 NW 12th Ave, JMH WW 279, Miami, FL 33136, USA.
E-mail address: tsubhawong@miami.edu (T.K. Subhawong).
[1] These authors contributed equally to this work

https://doi.org/10.1016/j.ejro.2022.100422
Received 5 February 2022; Received in revised form 14 April 2022; Accepted 16 April 2022
Available online 25 April 2022
2352-0477/© 2022 The Author(s). Published by Elsevier Ltd. This is an open access article under the CC BY-NC-ND license (http://creativecommons.org/licenses/by-nc-nd/4.0/).

glucose and is particularly sensitive for malignancy based on its accumulation in cancer cells where glycolysis is preferentially enhanced [6]. The CT component of the exam allows for accurate anatomic localization of functional tumors as well as attenuation correction of radiotracer avidity [7]. While not universal, intravenous iodinated contrast may be administered to further improve the diagnostic quality of the CT component of the exam[8]. Respiratory motion artifacts introduced by shallow breathing during PET/CT image acquisition partially obscure small subcentimeter pulmonary nodules [9], but quantitative assessment of metabolic activity in nodules is accurate in diagnosing malignancy in nodules down to 8 mm [10]. As such, PET/CT serves as a backbone of oncologic imaging.

However, routine surveillance PET/CT inevitably increases cumulative radiation exposure, of particular concern in hereditary cancer syndromes where screening may begin in childhood or adolescence, and where ionizing radiation should be minimized given patients' particular genetic susceptibilities to radiation-induced cancers [11,12]. Whole-body MRI (WB-MRI) offers a non-ionizing imaging modality to screen for lesions and assess disease extent in a single integrated examination, and is thus ideally suited for serial surveillance exams in cancer predisposition syndromes. Greater utilization of WB-MRI has accompanied increased access to more advanced MRI systems with improvements in acquisition speed and quality, and increased awareness of its applications. In the pediatric population specifically, the lack of ionizing radiation in WB-MRI is the greatest reason for its popularity [13]. Recent prospective data has shown WB-MRI to be a cost-effective and time-reducing tool in staging of newly diagnosed non-small-cell lung cancer [14], and it seems reasonable to expect a streamlined WB-MRI screening strategy would also benefit patients with hereditary cancer syndromes. The elements of the WB-MRI protocol at our institution are listed in Table 2.

Impediments to widespread WB-MRI implementation include variation in machine protocol and acquisition parameters, radiologist experience in interpretation, and lack of uniform reporting structure. Petralia et al. recently published guidelines- Oncologically Relevant Findings Reporting and Data System (ONCO-RADS)– to address some of these concerns, emphasizing a standard framework for categorizing abnormal findings so that risk stratification for malignancy can be better communicated [15]. For WB-MRI, younger children need to be sedated to ensure images are not degraded by motion artifacts [16]. Finally, for patients in the United States with private insurance, there is no consensus on the correct Current Procedural Terminology (CPT) medical billing code to use for WB-MRI. Many centers may submit under one of three codes, "unlisted MRI," "MRI chest/abdomen/pelvis," or "MRI bone marrow evaluation," yet none of these codes fully and adequately encapsulate the complexity of the exam as performed in practice [17].

3. Hereditary cancer syndromes

3.1. Neurofibromatosis type I (NF1)

Neurofibromatosis type 1 (NF1) is caused by pathogenic variants in the tumor suppressor gene *NF1*. It is characterized by multiple neurofibromas (NFs), which can be plexiform and associated with soft tissue overgrowth called elephantiasis neuromatosa (Fig. 1) [18]; abnormal skin pigmentation (café-au-lait spots, and freckling in the axillary or

Table 1
Common cancers and other manifestations of hereditary cancer syndromes.

Hereditary Cancer Syndrome (OMIM #)	Gene (s) (OMIM #)	Common Tumors/Cancers	Other Common Manifestations
Neurofibromatosis type I (NF1) (162200)	*NF1* (*613113)	Cutaneous neurofibromas, Lisch nodules (pigmented iris hamartomas), optic gliomas, pheochromocytomas	Café-au-lait spots, intellectual disability
Neurofibromatosis type II (NF2) (101000)	*NF2* (*607379)	Bilateral vestibular schwannomas, meningioma, ependymomas	Juvenile cataracts
Lynch syndrome (120435)	*MLH1* and *MSH2* (*609309)	Colorectal cancer, endometrial cancer	Ovarian, small bowel, and gastric adenocarcinoma; urothelial carcinoma
Hereditary breast and ovarian cancer (HBOC) syndrome (604370/612555)	*BRCA1, BRCA2* (*113705/ *600185)	Breast cancer, ovarian cancer	Primary peritoneal serous carcinoma, fallopian tube serous carcinoma, pancreatic ductal adenocarcinoma, colon and prostate cancers
Familial adenomatous polyposis (FAP) (175100)	*APC* (*611731)	Colorectal cancer, colonic adenoma	Papillary thyroid; duodenal adenocarcinoma; brain tumors; hepatoblastoma; Desmoid-type fibromatosis
Von Hippel Lindau (VHL) disease (193300)	*VHL* (*608537)	Central nervous system hemangioblastoma, RCC	Pheochromocytoma, endolymphatic sac tumors, papillary cystadenoma of epididymis
Tuberous sclerosis (191100/613254)	*TSC1, TSC2* (*605284/ *191092)	Cortical tubers; subependymal giant cell astrocytoma (SEGA); PEComas: renal angiomyolipoma, and pulmonary lymphangiomyomatosis (LAM) in women	Disorders of neuronal migration, cardiac rhabdomyoma
Li-Fraumeni syndrome (LFS) (151623)	*P53* (*191170)	Osteosarcoma and other sarcomas, breast cancer	Adrenocortical carcinoma, brain tumors, leukemia
Multiple Endocrine Neoplasia Type 1 (MEN1) (131100)	*MEN1* (*613733)	Parathyroid adenoma, pancreatic and duodenal neuroendocrine tumors	Pituitary adenoma
Multiple Endocrine Neoplasia Type 2 (MEN2) (171400/162300)	*RET* (*164761)	Medullary thyroid cancer (MTC), pheochromocytoma	Parathyroid adenoma
Birt-Hogg Dube (BHD) syndrome (135150)	*FLCN* (*607273)	Renal tumors: oncocytoma, hybrid oncocytic tumors, and chromophobe RCC Lung cysts	Fibrofolliculoma: benign hair follicle tumor
Cowden syndrome (158350)	*PTEN* (*601728)	Breast cancer, papillary thyroid cancer	Papillary RCC, endometrial and colorectal cancers
Hereditary paraganglioma-pheochromocytoma (PGL) syndromes (168000/115310)	*SDHD, SDHB, SDHC, D-HAF2* (*602690/ *185470)	Paraganglioma, pheochromocytoma	Gastrointestinal stromal tumor (GIST)
Multiple Hereditary Exostoses (MHE) (133700/133701)	*EXT1, EXT2* (*608177/ *608210)	Osteochondroma, chondrosarcoma	

Table 2
Whole-Body MRI Protocol.

No.	Sequence	Plane	TR/TE	Slice thickness (mm)	FOV (cm)	Matrix	Acquisition time (per station)
1	T1-weighted	Coronal	TR/TE 450/11 ms	6	40	256 × 180	2:06
2	STIR	Coronal	TR/TE/TI 3570/61/220 ms	6	40	256 × 180	2:31
3	VIBE Dixon (fat, water, in-phase and opposed-phase)	1) Coronal 2) Sagittal reformatted through spine	TR/TE1 and TE2 6.6/1.3 and 2.5 ms, flip angle 9^0	1.5	40	256 × 230	0:57
4	T2 HASTE	Coronal	TR/TE 1800/109 ms, flip angle 120^0	6	40	320 × 320	1:12
5	DWI, 2 b-values at 50 and 800 s/mm^2	Axial	TR/TE/TI 8720/60/240 ms	5	43	134 × 134	3:56

Table 2. Whole-body MRI protocol at 3 T. The protocol entails imaging vertex to knees, in multiple stations that undergo adaptive inline composing to generate images of the entire body; the total acquisition is approximately 1 h. STIR: short-tau inversion recovery; VIBE: volumetric interpolated breath-hold examination; HASTE: Half-Fourier single-shot turbo spin-echo; DWI: diffusion-weighted imaging; FOV: field of view; TR: repitition time; TE: echo time; TI: inversion time.

Fig. 1. 12-year-old male with NF1 and plexiform neurofibroma involving the tibial nerve (arrows), that has been described as resembling a "bag of worms". There is enlargement and edema-like signal throughout the overlying skin and soft tissues (*), termed "elephantiasis neuromatosa." This soft tissue overgrowth is thought to be due to a combination of a neoplastic proliferation of the perineural connective tissues, congenital lymphatic insufficiency, and chronic hyperemia.

inguinal regions); and/or iris hamartomas (Lisch nodules). The most common neoplasms associated with NF1 are malignant peripheral nerve sheath tumors (MPNST), optic gliomas, and brain tumors. There is also an increased risk for breast, neuroendocrine, and genitourinary tumors [19].

There is no consensus on the frequency or modality of surveillance imaging for brain tumors or MPNST in NF1. ^{18}F-FDG PET has shown decent accuracy in distinguishing MPNST from benign neurofibromas, with reported sensitivity of 91% and specificity of 84%; early (1 hr) and delayed (4 hr) acquisition protocols showed comparable accuracy [20]. Regarding regional MRI, some strategies rely on MRI surveillance of asymptomatic tumors while a more conservative approach entails using MRI only for the investigation of symptomatic tumors [21]. Regional MRI for plexiform NF is probably justified to establish baseline anatomic extent and to monitor atypical neurofibromas, which presumably represent precursor lesions to MPNST [22]. One approach recently advocated at a high-volume center utilized WB-MRI with diffusion -weighted imaging (DWI) and apparent diffusion coefficient (ADC) mapping in "high-risk" patients (Fig. 2), defined as those with *NF1* gene microdeletion, family or personal history of atypical NF or MPNST, prior radiation therapy, or high internal PNST burden [22]. High total tumor burden has been associated with increased risk for MPNST development; other imaging biomarkers of MPNST risk include low ADC values ($<$1.0 mm^2/s), large size, and internal tumor architecture and heterogeneity (distinct nodular zones) [22–24].

Women with NF1 have a higher risk of developing breast cancer before the age of 50 [25,26]. Surveillance for breast cancer in this population includes an annual mammogram starting at age 30 [27]. It is recommended to perform annual breast MRI, in addition to mammograms between the ages of 30–50 years old. Lastly, neuroendocrine neoplasms are also common in NF1 patients, and screening for pheochromocytoma is suggested to begin at age 18 with plasma or urine free fractionated metanephrines every one to two years [28].

3.2. *Neurofibromatosis type II (NF2)*

Neurofibromatosis type 2 (NF2) is an autosomal dominant syndrome that results from pathogenic variants in the tumor suppressor gene NF2. The most distinctive feature of NF2 is bilateral vestibular nerve schwannomas (Fig. 3), although patients are also predisposed to the development of lesions of the skin, eyes, and nervous system. Other tumors associated with NF2 include meningiomas, astrocytomas, ependymomas, and retinal hamartomas. Malignant degeneration into MPNSTs among NF2 patients appears restricted to those who have been irradiated [29].

Penetrance is nearly 100% by the age of 60. Affected and at-risk individuals should be screened yearly for ophthalmic or neurological findings and should have audiology evaluation An annual cranial MRI and spinal MRI starting at 10 years of age until at least age 40 is also recommended as part of the screening protocol [30]. WB-MRI currently is not a standard screening method for NF2. However, it has a role in assessing tumor burden and characterizing neoplasms that drive morbidity. WB-MRI has been used to evaluate tumor treatment response (by volume) in some NF2 clinical trials [22]. Regarding the use of ^{18}F-FDG PET/CT in detecting tumors in NF2, imaging features overlap as benign PNSTs have high metabolic activity and ^{18}F-FDG uptake, mimicking malignancy [22]. However, since NF2 schwannomas lack the predisposition to malignancy seen in NF1 PNSTs, whole body *surveillance* imaging is disputable [22].

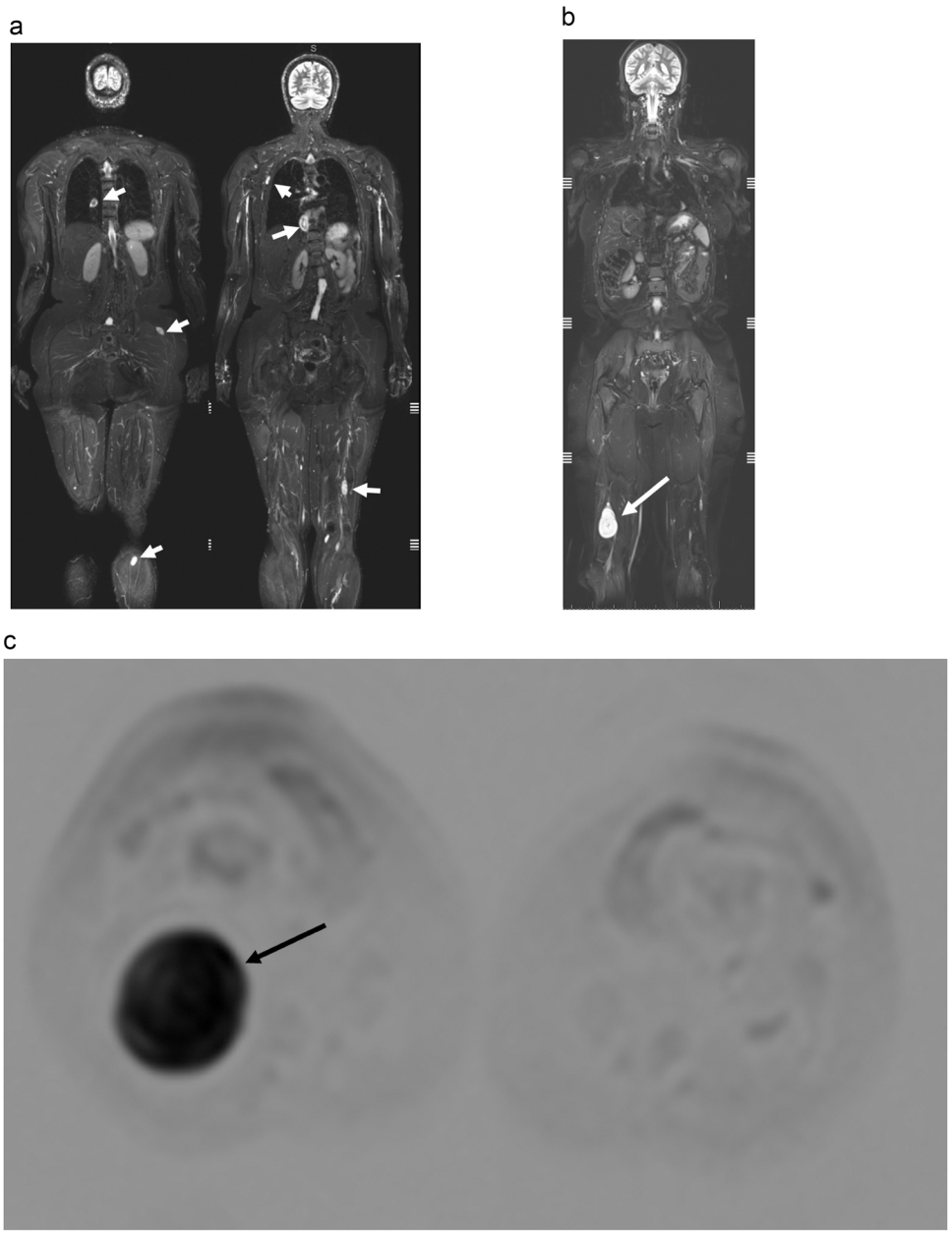

Fig. 2. Whole body MRI (WB-MRI) in patients with NF1. A) WB-MRI coronal STIR composite images in 50-year-old woman show multiple neurofibromas (arrows). B) WB-MRI coronal STIR in a 21-year-old woman with history of MPNST in left foot status post below knee amputation (not shown), undergoing surveillance scanning demonstrating a benign PNST in the right popliteal fossa (arrow). C) Axial DWI (b-800) shows the PNST (arrow) with increased diffusion, mean ADC value measured 1.6×10^{-3} mm^2/s; higher ADC values are more likely in benign tumors compared to MPNST.

3.3. Lynch syndrome (LS)

Lynch is the most common hereditary cancer syndrome, accounting for up to 3% of newly diagnosed colorectal cancer cases. It is an autosomal dominant disorder caused by defects in DNA mismatch repair genes (*MLH1*, *MSH2, MSH6, PMS2* or deletion of *EPCAM* causing transcriptional read-through silencing of *MSH2*). Among the various extracolonic malignancies associated with Lynch syndrome, endometrial cancer is the most common. The lifetime cumulative risk of endometrial cancer for women with Lynch syndrome is 40–60% [31]. The lifetime risk for ovarian cancer in women with Lynch syndrome is ~8% [32]. Other extracolonic malignancies associated with Lynch syndrome are transitional cell carcinoma of the urinary tract; adenocarcinoma of the stomach (Fig. 4), hepatobiliary tract, and small bowel malignancies; glioblastoma; prostate adenocarcinoma; and sebaceous neoplasms of the skin [33]. Studies show an association with sarcoma, and an increased risk for breast cancer in families with Lynch syndrome.

Screening recommendations include annual or biennial colonoscopy beginning at age 20–25 years of age, or 2–5 years before the youngest diagnosis in the family, whichever comes first. For women, an annual pelvic exam, transvaginal ultrasound, and an endometrial sample should be completed starting at the age of 30–35 years [34], though proof of survival benefit from endometrial surveillance has been elusive [33]. The US Multi-Society Task Force on Colorectal Cancer encouraged an annual transvaginal ultrasound to screen for ovarian cancer in women with LS beginning at age 30–35 years. While the panel advised against routine screening for small bowel cancers, annual esophagogastroduodenoscopy to screen for gastric cancer was recommended to start at age 30–35 years [33]. Solid evidence to support routine screening with ultrasound or CT of the urinary tract is lacking, though CT urogram is indicated for hematuria work-up in this patients [33]. Inconsistent data on whether LS patients are at substantially elevated risk for cancers of the prostate and breast generally fail to warrant more intensive screening programs beyond those already recommended for the general population. However, emerging data on patients with *PMS2* mutations suggest a heightened breast cancer risk that may deem them eligible for

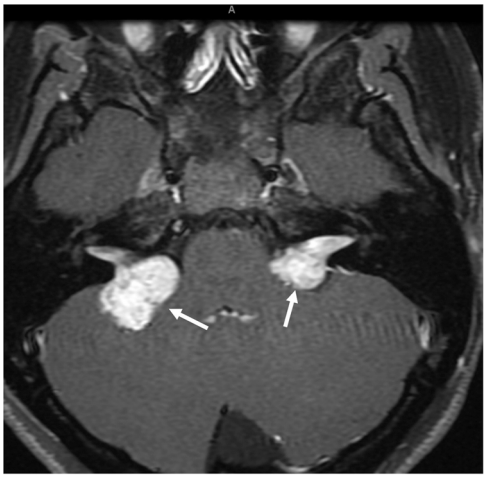

Fig. 3. 19-year-old female with bilateral enhancing vestibular schwannomas (arrows), characteristic of NF2.

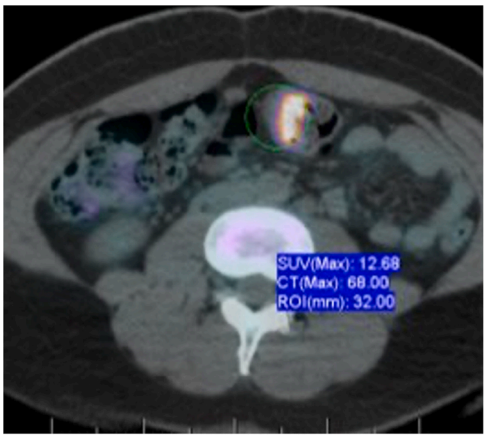

Fig. 4. 42-year-old African American woman with Lynch syndrome MSH2 (Muir-Torré syndrome variant), showing an FDG-avid (SUVmax 12.7) T3 adenocarcinoma in transverse colon, detected during staging PET-CT performed subsequent to diagnosis of scalp sebaceous carcinoma.

MRI surveillance [35]. For less common cancers involving the pancreas, biliary tract, and brain, there is no defined role for routine screening. Some authors have proposed WB-MRI for screening in this population, but this has not been widely adopted in consensus guidelines [13].

3.4. Hereditary breast and ovarian cancer (HBOC) syndrome

Hereditary breast and ovarian cancer syndrome (HBOC) accounts for 10–12% of all breast cancers. More than 50% of HBOC is due to pathogenic germline mutations in *BRCA1* and *BRCA2* – located on chromosomes 17 and 3, respectively. The cumulative risk of breast cancer by age 80 is 72% in *BRCA1* carriers and 69% in *BRCA2* carriers. The cumulative risks of ovarian cancers by age 80-year-old are 44% and 17% for *BRCA1* and *BRCA2*, respectively [36].

The recommended screening for HBOC syndromes includes annual breast MRI (or mammogram with consideration of tomosynthesis only if MRI is not available) starting at age 25–29 years [36]. Annual mammography in combination with breast MRI is recommended from age 30–75 years of age. Due to the increased risk of developing interval cancers, alternating MRI and mammographic screening at 6-month intervals has been proposed to make earlier detection possible [2]. This is 10–15 years before the American Cancer Society and European reference Network (ERN) for Genetic Tumor Risk Syndromes (GENTURIS) recommended ages for average-risk women to initiate annual screening mammography [37]. There is significant heterogeneity in screening strategies based on geography and institutional norms, but one common approach is to stagger mammograms and MRI at 6-month intervals. Screening ultrasound is utilized in a minority of centers [38] and its role as a primary modality is not yet established.

Ovarian cancer screening is controversial, with limited data supporting a combination of transvaginal ultrasound, serial serum CA-125 levels, and risk of ovarian cancer algorithm (ROCA) screening [39]. Other studies have failed to show that ovarian cancer screening strategies are efficacious in achieving survival benefits [39]. The availability of a screening option may deter patients from risk-reducing bilateral salpingo-oophorectomy (RRSO), which does have proven survival benefit [40]. It is also unnecessary to conduct imaging surveillance for peritoneal cancer after RRSO [41].

3.5. Familial adenomatous polyposis (FAP)

Familial adenomatous polyposis (FAP) is an autosomal dominant cancer predisposition syndrome caused by the pathogenic germline variants in *APC* gene [42]. FAP is one of the "*APC*-associated polyposis conditions" characterized by more than 100 adenomatous colonic polyps. Other *APC*-associated polyposis conditions are attenuated FAP, and gastric adenocarcinoma and proximal polyposis of the stomach FAP. Up to 50% of patients with FAP develop colonic adenomas by age 15. If not treated with a prophylactic colectomy, the lifetime risk of colorectal cancer is 100% in affected individuals [43,44]. Previously accepted terms such as Gardner syndrome (FAP with osteomas and desmoid tumors) and Turcot syndrome (FAP with CNS tumors including medulloblastoma or glioblastoma) are not used and considered as APC spectrum [45].

Imaging is not the primary tool in FAP monitoring, but in patients with previously unknown FAP, tumors may first be discovered on CT, MR, or PET/CT, facilitating detection, management, and future surveillance of this condition. In patients with known FAP, annual colonoscopy should begin around age 10 and an upper GI endoscopy is recommended between the ages of 25 and 30, with continued interval screening between six months to four years [34]. Prophylactic colectomy is mandatory, with surgical options including proctocolectomy with end ileostomy, subtotal colectomy with ileorectal anastomosis (IRA), and colectomy with an ileal pouch-anal anastomosis (IPAA). After surgical intervention, cancer may still arise in the remaining rectal stump [46]. Following a colectomy/IPAA/IRA, there is an increased risk of adenomas in the ileum, rectal cuff, and anal transition zone, necessitating continued surveillance. Specifically after an IPAA, the American Society for Gastrointestinal Endoscopy recommends a pouch endoscopy 1 year after surgery and subsequent endoscopies every 1–2 years, or every 6 months if an advanced adenoma is detected [47]. Following an IRA, a sigmoidoscopy is recommended 6 months after surgery, followed by surveillance every 6 months to one year [47]. Similar recommendations were developed throughout Europe in February 2007 during a workshop in Mallorca by European experts on hereditary gastrointestinal cancer [48]. Post-colectomy morbidity and mortality in patients with FAP are mostly due to desmoid-type fibromatosis (DF) developing in the mesentery (Fig. 5), and duodenal cancer [49]. DF tumors are intermediate, locally aggressive mesenchymal neoplasms which, while lacking the ability to metastasize, may cause substantial morbidity and mortality due to relentless infiltrative growth [50]. DFs in FAP typically arise in the mesentery and display characteristic infiltrative tails of tumor extending into adjacent fat and encasing bowel; MRI reveals heterogeneous T2 hyperintensity and enhancement reflect a fibroblastic cellular parenchyma admixed with hypointense bands of collagen [51]. With systemic therapy, DF often shows increased collagenization and corresponding decreased T2 signal intensity that precedes tumor shrinkage [52]. Aside from DF, surveilling for extra-gastrointestinal lesions in FAP patients is only weakly recommended [49].

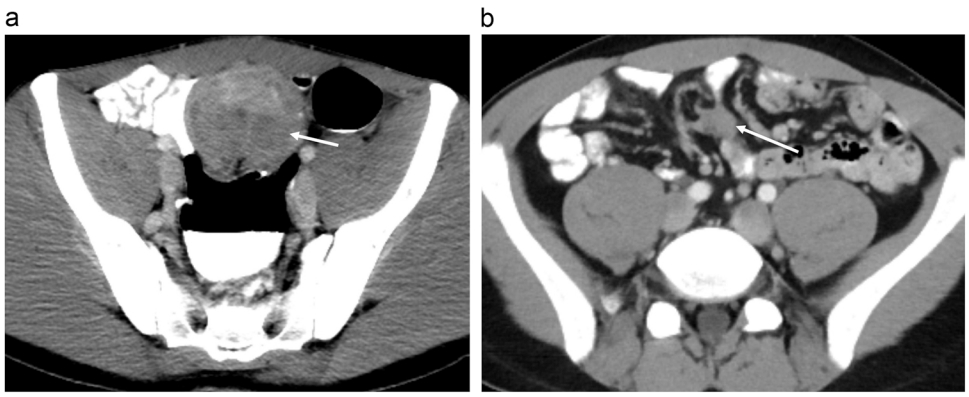

Fig. 5. 23-year-old man with FAP status post total colectomy at age 19, with 6 cm mesenteric desmoid-type fibromatosis in the lower abdomen (arrow). The patient had a good response to sorafenib initially but was switched after several months to NSAIDs due to toxicity. B) Seven years later, the desmoid tumor (arrow) shows a dramatic decrease in size. Various systemic therapies are active in the treatment of desmoid-type fibromatosis.

3.6. Von Hippel Lindau (VHL)

VHL disease is an autosomal dominant syndrome driven by germline mutations in the *VHL* tumor suppressor gene. CNS hemangioblastomas are the most common tumor in VHL affecting the brain, spinal cord, and retina (Fig. 6). These neoplasms commonly present during adulthood, but screening and surveillance for patients with VHL should begin in childhood [53]. The lifetime risk of developing clear cell renal cell carcinoma (RCC) is close to 70%, and pheochromocytomas may occur in up to 20% of patients with VHL [54].

Clinical screening consists of optic, neurologic, and audiology testing beginning early in childhood, accompanied by an annual analysis of metanephrine levels starting at five years of age [53]. Biennial contrast-enhanced MRI of the brain and spine to screen for hemangioblastomas is recommended starting at age 11 years [55]. This may include thin slices with high resolution to assess for endolymphatic sac tumors. Abdominal MRI annually or at least biennially is also recommended beginning at the age of 15 to assess the pancreas, kidneys, and adrenals [53,55].

Recently, a 35-minute WB-MRI screening protocol tailored to detect VHL-specific lesions in the brain, spine, and abdomen with a single dose of gadolinium (Gd) was proposed to replace multiple separate contrast-enhanced MRI examinations of different body regions, without compromising lesion conspicuity [56]. From January 2016 to November 2018, this one-step WB-MRI approach was used successfully in 18 VHL patients, showing all lesions detected on the previous conventional MRI scans of the same patients [56]. Another surveillance option being explored is ^{68}Ga-DOTATATE PET/CT, which may have higher sensitivity for neuroendocrine tumors than conventional CT or MRI [57], but additional data are needed to better define its role in routine screening.

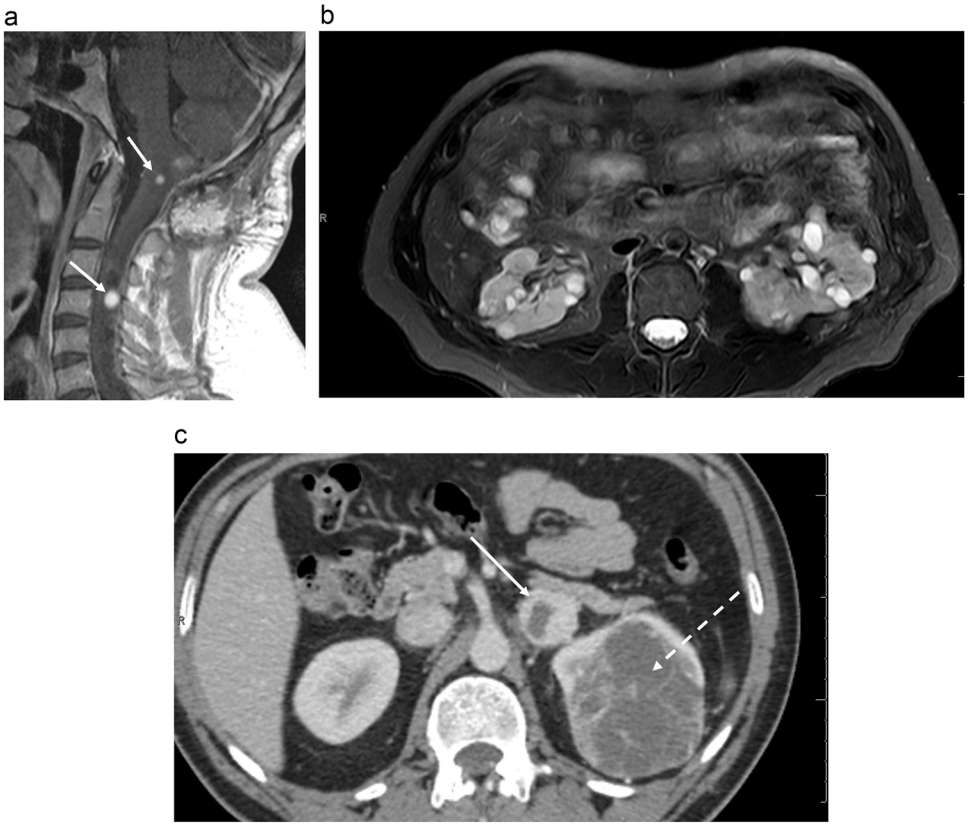

Fig. 6. A) 34-year-old man with von Hippel Lindau; sagittal post-contrast T1-weighted MRI of the cervical spine demonstrates multiple enhancing hemangioblastomas in the medulla and proximal cord. B) Axial fat-suppressed T2-weighted MRI of his abdomen demonstrates polycystic kidney disease. C) 43-year-old man with VHL (different patient than in A and B), with arterial phase contrast-enhanced CT showing a left adrenal pheochromocytoma (solid arrow) and grade 3 clear cell renal carcinoma (dashed arrow).

3.7. Tuberous sclerosis (TS)

Tuberous sclerosis (TSC) is a rare, autosomal dominant neurocutaneous disorder characterized by the development of non-cancerous tumors in the brain and other essential organs such as the kidneys, lungs, heart, eyes, and skin. It is caused by pathogenic variants in the tumor suppressor genes *TSC1* or *TSC2*. Patients diagnosed with TSC can show signs of the disease as early as one-year of age. While the classic diagnostic Vogt triad consists of seizures, impaired cognition, and facial angiofibromas, the clinical presentation can be highly variable. In addition to brain lesions, other involved organs include heart (cardiac rhabdomyomas), lung (lymphangioleiomyomatosis (LAM)), kidney (angiomyolipomas, AML, RCCs) (Fig. 7), skin, and eyes (e.g. retinal Lisch nodules) [58].

The distinguishing brain findings in patients with TSC include subependymal nodules, cortical and subcortical tubers (Fig. 8), gray matter heterotopia, and subependymal giant cell astrocytomas (SEGAs) which occur in late childhood in 10–15% of patients [58]. A recent literature review established fetal MRI detection rates for subependymal nodules and cortical/subcortical lesions at approximately 60% and 37%, respectively [59]. Prenatal diagnosis of such abnormalities has prognostic significance, as total lesion burden is associated with delays in cognitive and motor development, and with autism spectrum disorder 33640330 [60]. Surveillance contrast enhanced brain MRI is recommended every 1–3 years until the patient is 25 years old, with continued surveillance needed only if SEGAs are present [61–63].

The vast majority (~95%) of renal AMLs show evidence of internal fat on CT and MRI and are correspondingly echogenic on ultrasound. Renal AMLs may spontaneously bleed or rupture, especially when large (>4 cm) or quickly growing, resulting in the second most common cause of morbidity among TSC patients [58]. Lifelong follow-up with abdominal MRI every 1–3 years is recommended, and for asymptomatic enlarging AMLs > 3 cm, mTOR inhibitors are the recommended front-line therapy [63].

Fig. 8. 45-year-old man with tuberous sclerosis. Axial FLAIR MRI shows multiple cortical and triangular shaped subcortical tubers (arrows); these lesions represent glioneuronal hamartomas and can be epileptogenic. Also present are radial bands (arrowheads); while the exact pathogenesis of the bands remains uncertain, it is likely related to dysfunction in neuronal migration.

Cardiac rhabdomyoma is often the first radiologic finding in TSC, and can be detected on fetal ultrasound between 20 and 30 weeks gestation [64]; fetal MRI is also highly sensitive, particularly with increasing gestional age, and may reveal cardiac rhabdomyoma in up to 94% of examinations [59]. Spontaneous regression is observed in up to

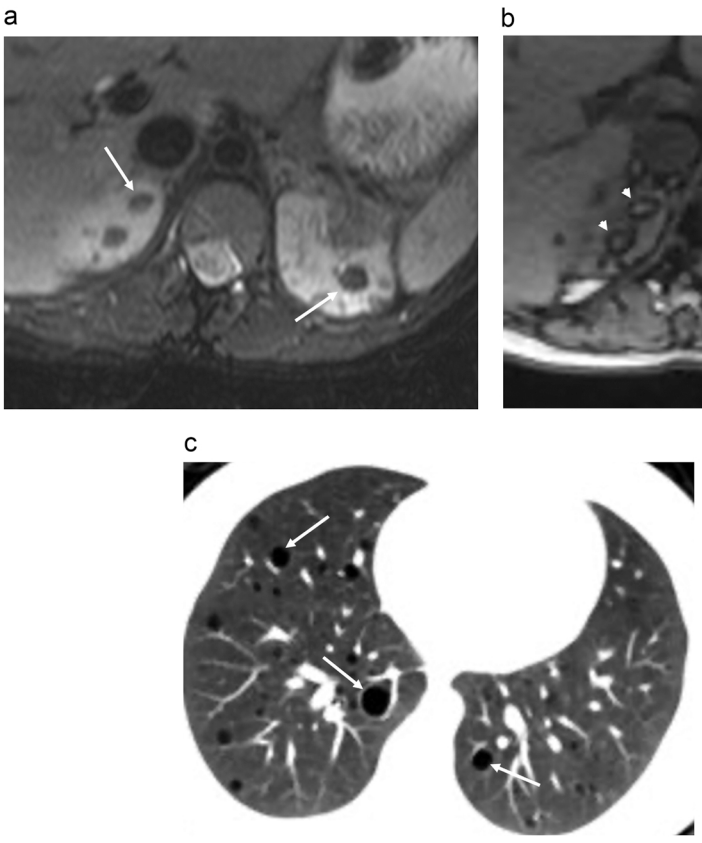

Fig. 7. 40-year-old woman with tuberous sclerosis. A) Axial T2 fat-suppressed MRI shows multiple fatty renal masses in the upper poles of both kidneys (arrows), consistent with angiomyolipomas. B) Chemical shift imaging demonstrates "India ink" artifact at the mass boundaries (arrowheads) due to signal drop at the water-fat interface on the opposed-phase sequence. C) Axial chest CT depicts the pulmonary manifestation of lymphangioleiomyomatosis (LAM) as variably sized smooth-walled cysts of resulting from destruction of lung parenchyma. Both AML and LAM are perivascular epithelioid cell tumors (PEComas).

70% of patients by age 4, but surveillance to resolution is recommended as rare serious complications such as heart failure, valvular dysfunction, and arrhythmia can occur [58,64].

Like renal angiomyolipoma, LAM is a type of perivascular epithelioid cell tumor (PEComa) and occurs in up to approximately 50% of patients, leading to dyspnea, cough, pneumothorax, and chylothorax [58]. High-resolution chest CT surveillance should be performed every 5–10 years in asymptomatic TSC patients without LAM at baseline, and every 2–3 years once detected, though more nuanced surveillance may be influenced by patient-specific factors [58,63].

3.8. Li-Fraumeni syndrome (LFS)

Li-Fraumeni Syndrome (LFS) is an autosomal dominant cancer predisposition syndrome caused by a germline pathogenic mutation in the tumor suppressor gene *TP53*. In patients with LFS, particularly close monitoring for osteosarcoma and other sarcomas (Fig. 9), breast cancer, adrenocortical carcinoma, leukemias, and tumors of the central nervous system is recommended. In a landmark prospective trial study, Villani et al. showed that a biochemical and imaging surveillance strategy (whole-body MRI, brain MRI, breast MRI, mammography, abdominal and pelvic ultrasound, and colonoscopy) resulted in superior 5-year overall survival in patients who received screening imaging versus those who did not (89% vs 60%) [3].

Current international consortium protocols recommend that patients with the LFS-associated gene mutation should undergo abdominal ultrasounds every 3–4 months up to age 10-year-old, as well as annual WB-MRI and annual brain MRI with contrast throughout their entire lives [65,66]. The consortium also recommends annual breast MRI for women 20 years of age and older, with risk-reducing mastectomy discussed with patients on an individual basis. Through WB-MRI screening, it has been estimated that new and localized primary cancers resulting from the mutation of LFS may be detected at a rate of nearly 7%, providing evidence of high utility of such screening in this patient population [65]. Given the broad range of potential malignancies resulting from the LFS germline mutation, many have emphasized avoiding ionizing radiation screening methods, such as CT and PET/CT, to allow for maximization of imaging frequency while also mitigating imaging-related radiation-induced cancer acceleration risks [67]. In a study by Anupindi in 2015, WB-MRI was 100% sensitive and 94% specific in detecting cancer in children with LFS, paraganglioma-pheochromocytoma syndrome, or rhabdoid tumor syndrome [67].

Fig. 9. 47-year-old woman with Li Fraumeni; axial contrast-enhanced fat-suppressed T1-weighted MRI demonstrates a 3 cm heterogeneously enhancing mass in the deep masticator space, which was a recurrent grade 3 myofibrosarcoma.

3.8.1. Multiple endocrine neoplasia (MEN) syndromes, types 1 & 2

Multiple endocrine neoplasia (MEN) syndromes are autosomal dominant cancer predisposition syndromes associated with neuroendocrine tumors (NETs). MEN type 1 (MEN1) is caused by defects in the *MEN1* tumor suppressor gene, and is associated with adrenocortical adenomas, collagenomas, lipomas, and facial angiofibromas. The most common causes of death in MEN1 are duodenopancreatic NETs followed by thymic NETs [68]. The most common pancreatic NETs are nonfunctioning, affecting 55% of MEN1 patients, while functional NETs are observed in 20–50%, (most commonly gastrinomas and insulinomas) (Fig. 10). Accordingly, a focus on structural imaging with contrast-enhanced MRI or endoscopic ultrasound as the preferred initial screening modalities has been advocated, with annual screening starting at age 8; MRI has the added benefit of being able to assess for adrenocortical tumors [68]. Pituitary tumor screening should include dedicated pituitary protocol MRI every 3 years, as early as age 5, and surveillance of the chest for thymic and bronchopulmonary NETs should be carried out by CT or MRI annually, starting at age 15. The role of functional imaging in screening with ^{68}Ga-DOTATATE PET/CT, octreotide scanning, and ^{18}F-FDG PET/CT remains uncertain [68].

MEN type 2 (MEN2) is caused by gain-of-function mutations in the protooncogene *RET*. It has three different subtypes - MEN2A, MEN2B, and familial medullary thyroid cancer (FMTC). Patients with MEN2A manifest the phenotype between the ages of 5 and 25 years, including primary hyperthyroidism (15–30%), pheochromocytomas (>50%), and medullary thyroid carcinoma (MTC; 100%). Rarely, Hirschsprung disease and cutaneous lichen amyloidosis may also present in MEN2A patients. MEN2B may also result in the development of MTC in addition to neuromas, diffuse ganglioneuromatosis of the gastroenteric mucosa (40%), and presents with findings earlier than patients with MEN2A. Ultrasound, CT, PET/CT, and MRI have all demonstrated benefits in allowing physicians to identify nodal disease, local cancer invasion, and distant metastatic sites [61].

3.9. Birt-hogg-dube (BHD) syndrome

Birt-Hogg-Dube (BHD) syndrome is an autosomal dominant syndrome caused by defects in the tumor suppressor gene *FLCN*. It is associated with cutaneous fibrofolliculomas, multiple renal tumors, and bilateral pulmonary cysts (Fig. 11). Over 80% of BHD patients have variably sized pulmonary cysts that predominate in basilar and paramediastinal regions, and usually have thin uniform walls that are prone to rupture. The mean age of first pneumothorax is estimated between 36 and 38 years, and up to 5–10% of all patients with apparent spontaneous pneumothorax are thought to have BHD [69]. In rare cases, lung cysts

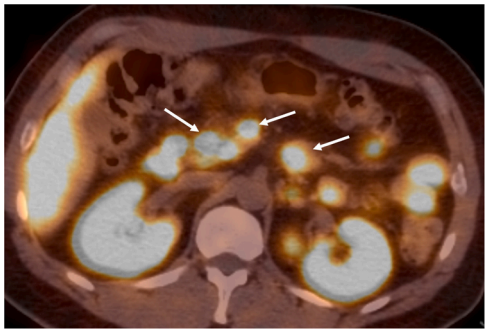

Fig. 10. 46-year-old man with MEN1. Axial fused image from ^{68}Ga-DOTATATE PET/CT reveals multiple focal lesions with intense radiotracer uptake in the pancreas (arrows), indicative of functional pancreatic neuroendocrine tumors.

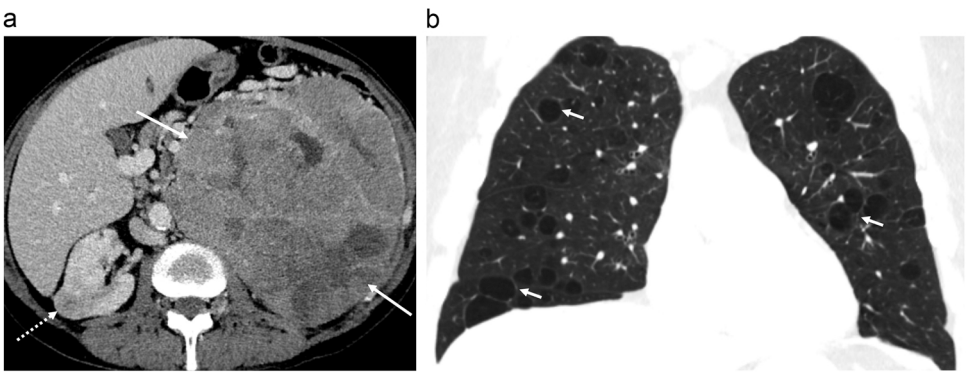

Fig. 11. A) 66-year-old man with Birt-Hogg-Dube. Axial contrast-enhanced CT demonstrates a large heterogeneous 20 cm mass obliterating the left kidney (arrows), proven on biopsy to be renal cell carcinoma. An additional right renal mass (dashed arrow) was noted but never biopsied as the patient was referred to hospice. B) 71-year-old man (different from A) with Birt-Hogg-Dube. Coronal chest CT shows innumerable cysts with thin walls; rupture of these cysts can lead to spontaneous pneumothorax.

may even be revealed on prenatal ultrasound [70]. Renal neoplasms, particularly chromophobe and hybrid oncocytic/chromophobe RCCs, and clear cell RCCs, may affect over 25% of BHD patients at a mean age of 50 years [71,72]. Current recommendations state that contrast-enhanced abdominal MRI should begin at age 20 to screen for renal tumors, with 3-year interval surveillance for life [61,69].

3.10. Cowden Syndrome (CS)

PTEN hamartoma tumor syndrome (PHTS), is another autosomal dominant cancer predisposition syndrome, also known as Cowden syndrome, and is caused by germline pathogenic variants in *PTEN*. PHTS presents with hamartomatous growth in multiple organs. Affected individuals face increased risks of papillary thyroid cancer, papillary RCC, endometrial cancer, breast cancer, and colorectal cancers. Annual screening through physical exam for breast and thyroid cancer is highly recommended, as well as annual renal ultrasound starting at age 40-year-old and repeated biannually thereafter. Screening for endometrial cancer and baseline colonoscopy at age 35–40 has also been advocated for. CT and WB-MRI may also have screening utility in this patient population, although current protocols do not address standards for their uniform implementation [62].

3.11. Hereditary paraganglioma-pheochromocytoma (PGL) syndromes

Hereditary paraganglioma-pheochromocytoma (PGL/PCC) autosomal dominantly inherited condition associated with caused by germline pathogenic variants in *MAX*, *SDHA*, *SDHAF2*, *SDHB*, *SDHC*, *SDHD*, or *TMEM127*. Affected individuals are predisposed to paraganglioma (PGL), pheochromocytoma (PCC), RCC, gastrointestinal stromal tumor (GIST) (Fig. 12), and pituitary adenoma [73,74].

Fig. 12. 12-year-old female with SDHB deficiency. Axial contrast-enhanced CT shows a solid mass along the lesser curvature of the stomach, which is partially filled with oral contrast. This gastrointestinal stromal tumor (GIST) measured up to 4.5 cm, with 7 mitoses per 50 high-powered fields.

Tumors distribute along the paravertebral axis from the base of the skull to the pelvis. PGLs in the head and neck are typically found at the carotid bifurcation (carotid body tumor), middle ear cavity (glomus tympanicum), jugular foramen (glomus jugulare), and adjacent to the vagus nerve (glomus vagale) [34]. These patients are also at elevated risk (up to 70%) for papillary thyroid cancer, gastrointestinal stromal tumor (GIST), and RCC [62].

Screening guidelines vary based on the underlying molecular cause and symptoms, and include appropriate biochemical and imaging screening. Given the non-negligible risk of radiation-induced malignancy in this population, there has been a recent emphasis on the role of MRI screening [73]: in one study, 23% (15/65) of asymptomatic SDHB carriers were identified as having SDHB-related disease: ten identified on the first surveillance scan (five abdominal, three thoracic, one head/neck PGL; and one GIST) and five on subsequent surveillance scan (one abdominal, one pelvic PGL, and three RCCs). WB-MRI standards have been conveyed by Greer, outlined as including neck-to-pelvis WB-MRI, alternating with chest-to-pelvis MRI and dedicated neck MRI every 24 months, starting at 6–8 years of age [13]. Other surveillance strategies have stretched intervals out to 18 months for abdominal MRI (and head and neck in SDHD carriers), and every third year for WB-MRI [74].

3.12. Multiple hereditary exostoses (MHE)

Multiple hereditary exostoses (MHE) are associated with *EXT1* and *EXT2* pathogenic variants and, as the name indicates, are marked by the presence of numerous osteochondromas involving both axial and appendicular skeleton (Fig. 13). Although the risk of malignant transformation to chondrosarcoma is low for each individual osteochondroma, the cumulative risk in MHE patients has been estimated to be up to 11% [75]. The majority (~75%) of transformation events occur between ages 20–40%, and 56% are in the pelvis and proximal femur [76]. WB-MRI is well-suited to detect thickening of the cartilaginous cap in transforming lesions: in a recent retrospective study of 62 patients followed for mean 4.6 years, WB-MRI detected three asymptomatic chondrosarcomas, showing 100% sensitivity over the study period [75]. While formal WB-MRI surveillance protocols have yet to be established [75], the limited data available suggests annual WB-MRI in patients 20–40 years old may be cost-effective [76].

4. Conclusions

Despite costs of whole-body imaging via CT, MR, or PET/CT, the risk of allowing heritable cancers to go undetected without imaging screening is substantial. Therefore, radiographic imaging should be considered as a standard component of screening and surveillance in patients with a family history of cancer or identified genetic markers of a heritable cancer susceptibility syndrome. Given the inherent nature of

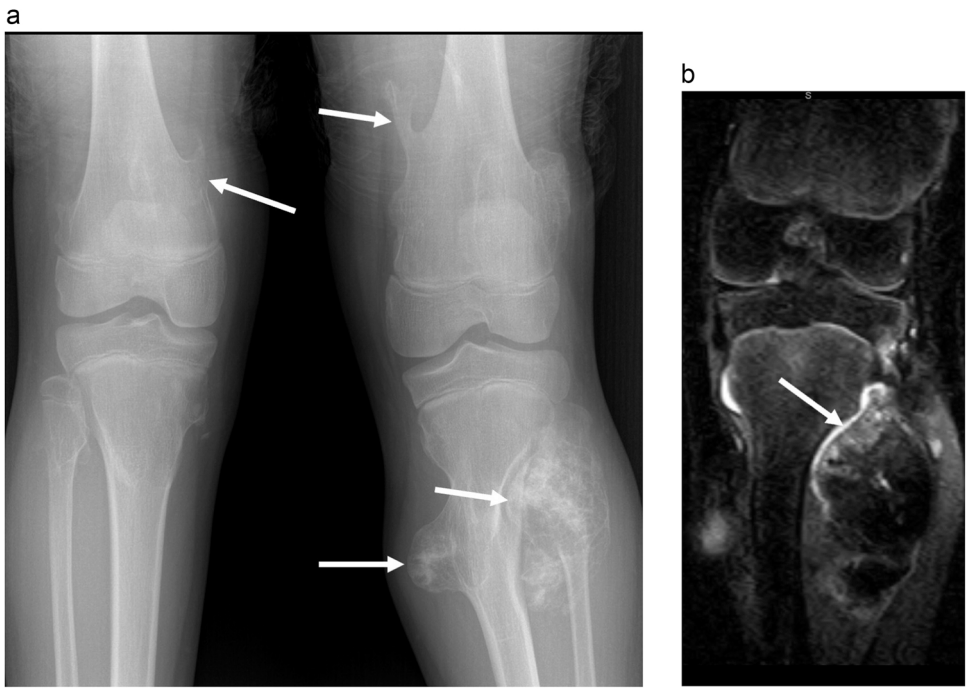

Fig. 13. 11-year old with multiple hereditary exostoses. A) AP radiograph of both knees shows numerous osteochondromas (arrows) arising from the widened long bone metaphyses bilaterally. B) Coronal STIR MRI shows a thin cartilage cap [36] of fibular osteochondroma causing remodeling of the proximal tibia. MRI permits detection in changes of the cartilage cap or perilesional edema, which can be markers of malignant transformation.

radiation exposure advancing risk of malignancy, WB-MRI may be of the most benefit in screening patients with hereditary cancer syndromes for cancer development and surveilling them for cancer progression. Further cohort studies are recommended to directly compare CT and PET/CT versus MR imaging in this population with regard to cost burden, risk of radiation exposure, and benefit of detecting gross atypia associated with the genetic predispositions in these patients.

Ethical approval details

not applicable.

Funding sources

none.

CRediT authorship contribution statement

Jamie E. Clarke: Conceptualization, Investigation, Visualization, Writing – original draft, Writing – review & editing. **Stephanie Magoon**: Conceptualization, Investigation, Visualization, Writing – original draft, Writing – review & editing. **Irman Forghani**: Conceptualization, Supervision, Writing – review & editing. **Francesco Alessandrino**: Conceptualization, Supervision, Writing – review & editing. **Gina D'Amato**: Conceptualization, Supervision, Writing – review & editing. **Emily Jonczak**: Conceptualization, Supervision, Writing – review & editing. **Ty K. Subhawong**: Conceptualization, Investigation, Project administration, Resources, Supervision, Validation, Visualization, Writing – review & editing.

Conflict of Interest

none.

References

[1] T.J. Perry, et al., The duty to warn at-risk relatives-the experience of genetic counselors and medical geneticists, Am. J. Med. Genet. A 182 (2) (2020) 314–321.
[2] P.P. Bharucha, et al., Genetic testing and screening recommendations for patients with hereditary breast cancer, Radiographics 40 (4) (2020) 913–936.
[3] A. Villani, et al., Biochemical and imaging surveillance in germline TP53 mutation carriers with Li-Fraumeni syndrome: 11 year follow-up of a prospective observational study, Lancet Oncol. 17 (9) (2016) 1295–1305.
[4] M.B. Daly, et al., NCCN guidelines insights: genetic/familial high-risk assessment: breast, ovarian, and pancreatic, Version 1.2020, J. Natl. Compr. Cancer Netw. 18 (4) (2020) 380–391.
[5] A. Mojtahedi, et al., The value of (68)Ga-DOTATATE PET/CT in diagnosis and management of neuroendocrine tumors compared to current FDA approved imaging modalities: a review of literature, Am. J. Nucl. Med. Mol. Imaging 4 (5) (2014) 426–434.
[6] J. Zheng, Energy metabolism of cancer: glycolysis versus oxidative phosphorylation (Review), Oncol. Lett. 4 (6) (2012) 1151–1157.
[7] A. Almuhaideb, N. Papathanasiou, J. Bomanji, 18F-FDG PET/CT imaging in oncology, Ann. Saudi Med. 31 (1) (2011) 3–13.
[8] S. Johnson, et al., Technical note on the administration of intravenous contrast media in hybrid imaging, Nucl. Med. Commun. 41 (7) (2020) 706–713.
[9] M. Allen-Auerbach, et al., Standard PET/CT of the chest during shallow breathing is inadequate for comprehensive staging of lung cancer, J. Nucl. Med. 47 (2) (2006) 298–301.
[10] J.R. Weir-McCall, et al., Impact of solitary pulmonary nodule size on qualitative and quantitative assessment using 18F-fluorodeoxyglucose PET/CT: the SPUTNIK trial, Eur. J. Nucl. Med. Mol. Imaging (2021) 1560–1569.
[11] B. Huang, M.W. Law, P.L. Khong, Whole-body PET/CT scanning: estimation of radiation dose and cancer risk, Radiology 251 (1) (2009), 166-74.
[12] J.R. Reid, L.J. States, Ionizing radiation use and cancer predisposition syndromes in children, J. Am. Coll. Radio. 15 (9) (2018) 1238–1239.
[13] M.C. Greer, Whole-body magnetic resonance imaging: techniques and non-oncologic indications, Pedia Radio. 48 (9) (2018) 1348–1363.
[14] S.A. Taylor, et al., Diagnostic accuracy of whole-body MRI versus standard imaging pathways for metastatic disease in newly diagnosed non-small-cell lung cancer: the prospective Streamline L trial, Lancet Respir. Med. 7 (6) (2019) 523–532.
[15] G. Petralia, et al., Oncologically relevant findings reporting and data system (ONCO-RADS): guidelines for the acquisition, interpretation, and reporting of whole-body MRI for cancer screening, Radiology 299 (3) (2021) 494–507.
[16] K. Darge, D. Jaramillo, M.J. Siegel, Whole-body MRI in children: current status and future applications, Eur. J. Radio. 68 (2) (2008) 289–298.
[17] R.V. Gottumukkala, et al., Current and emerging roles of whole-body MRI in evaluation of pediatric cancer patients, Radiographics 39 (2) (2019) 516–534.
[18] S. Bano, et al., Elephantiasis neuromatosa of the lower limb in a patient with neurofibromatosis type-1: a case report with imaging findings, J. Pedia Neurosci. 5 (1) (2010) 59–63.

[19] M. Zulfiqar, et al., Imaging features of neurofibromatosis Type 1 in the abdomen and pelvis, AJR Am. J. Roentgenol. 216 (1) (2021) 241–251.
[20] A. Chirindel, et al., 18F-FDG PET/CT qualitative and quantitative evaluation in neurofibromatosis type 1 patients for detection of malignant transformation: comparison of early to delayed imaging with and without liver activity normalization, J. Nucl. Med. 56 (3) (2015) 379–385.
[21] K.I. Ly, J.O. Blakeley, The diagnosis and management of neurofibromatosis type 1, Med. Clin. North Am. 103 (6) (2019) 1035–1054.
[22] S. Ahlawat, et al., Current status and recommendations for imaging in neurofibromatosis type 1, neurofibromatosis type 2, and schwannomatosis, Skelet. Radio. 49 (2) (2020) 199–219.
[23] C.S. Higham, et al., The characteristics of 76 atypical neurofibromas as precursors to neurofibromatosis 1 associated malignant peripheral nerve sheath tumors, Neuro Oncol. 20 (6) (2018) 818–825.
[24] S. Demehri, et al., Conventional and functional MR imaging of peripheral nerve sheath tumors: initial experience, AJNR Am. J. Neuroradiol. 35 (8) (2014) 1615–1620.
[25] O.O. Seminog, M.J. Goldacre, Age-specific risk of breast cancer in women with neurofibromatosis type 1, Br. J. Cancer 112 (9) (2015) 1546–1548.
[26] S.A. Madanikia, et al., Increased risk of breast cancer in women with NF1, Am. J. Med Genet A 158A (12) (2012) 3056–3060.
[27] H. Arem, et al., Quality of life among cancer survivors by model of cancer survivorship care, J. Psychosoc. Oncol. (2021) 1–13.
[28] Else, T., S. Greenberg, and L. Fishbein, Hereditary Paraganglioma-Pheochromocytoma Syndromes, in GeneReviews((R)), M.P. Adam, et al., Editors. 1993: Seattle (WA).
[29] D.G. Evans, et al., Identifying the deficiencies of current diagnostic criteria for neurofibromatosis 2 using databases of 2777 individuals with molecular testing, Genet Med. 21 (7) (2019) 1525–1533.
[30] S. Ardern-Holmes, G. Fisher, K. North, Neurofibromatosis type 2, J. Child Neurol. 32 (1) (2017) 9–22.
[31] L.A. Meyer, R.R. Broaddus, K.H. Lu, Endometrial cancer and Lynch syndrome: clinical and pathologic considerations, Cancer Control 16 (1) (2009) 14–22.
[32] K. Nakamura, et al., Features of ovarian cancer in Lynch syndrome (Review), Mol. Clin. Oncol. 2 (6) (2014) 909–916.
[33] F.M. Giardiello, et al., Guidelines on genetic evaluation and management of Lynch syndrome: a consensus statement by the US multi-society task force on colorectal cancer, Am. J. Gastroenterol. 109 (8) (2014) 1159–1179.
[34] R. Tiwari, et al., Radiologist's primer on imaging of common hereditary cancer syndromes, Radiographics 39 (3) (2019) 759–778.
[35] M. Sheehan, et al., Investigating the link between lynch syndrome and breast cancer, Eur. J. Breast Health 16 (2) (2020) 106–109.
[36] K.B. Kuchenbaecker, et al., Risks of breast, ovarian, and contralateral breast cancer for BRCA1 and BRCA2 mutation carriers, JAMA 317 (23) (2017) 2402–2416.
[37] D.H. Marmolejo, et al., Overview of hereditary breast and ovarian cancer (HBOC) guidelines across Europe, Eur. J. Med. Genet 64 (12) (2021), 104350.
[38] D. Madorsky-Feldman, et al., An international survey of surveillance schemes for unaffected BRCA1 and BRCA2 mutation carriers, Breast Cancer Res. Treat. 157 (2) (2016) 319–327.
[39] L. Andrews, D.G. Mutch, Hereditary ovarian cancer and risk reduction, Best. Pr. Res. Clin. Obstet. Gynaecol. 41 (2017) 31–48.
[40] M.G. Harmsen, et al., Very high uptake of risk-reducing salpingo-oophorectomy in BRCA1/2 mutation carriers: a single-center experience, Gynecol. Oncol. 143 (1) (2016) 113–119.
[41] M. Jacobson, et al., Risk reduction strategies for BRCA1/2 hereditary ovarian cancer syndromes: a clinical practice guideline, Hered. Cancer Clin. Pr. 19 (1) (2021) 39.
[42] W.F. Bodmer, et al., Localization of the gene for familial adenomatous polyposis on chromosome 5, Nature 328 (6131) (1987) 614–616.
[43] S. Bulow, Results of national registration of familial adenomatous polyposis, Gut 52 (5) (2003) 742–746.
[44] S. Bulow, Diagnosis of familial adenomatous polyposis, World J. Surg. 15 (1) (1991) 41–46.
[45] P. Dinarvand, et al., Familial adenomatous polyposis syndrome: an update and review of extraintestinal manifestations, Arch. Pathol. Lab. Med. 143 (11) (2019) 1382–1398.
[46] F.C. Gleeson, et al., Progression to advanced neoplasia is infrequent in post colectomy familial adenomatous polyposis patients under endoscopic surveillance, Fam. Cancer 8 (1) (2009) 33–38.
[47] J. Yang, et al., American society for gastrointestinal endoscopy guideline on the role of endoscopy in familial adenomatous polyposis syndromes, Gastrointest. Endosc. 91 (5) (2020) 963–982 e2.
[48] H.F. Vasen, et al., Guidelines for the clinical management of familial adenomatous polyposis (FAP), Gut 57 (5) (2008) 704–713.
[49] N. Tomita, et al., Japanese society for cancer of the colon and rectum (JSCCR) guidelines 2020 for the clinical practice of hereditary colorectal cancer, Int. J. Clin. Oncol. 26 (8) (2021) 1353–1419.
[50] D. Ganeshan, et al., Current update on desmoid fibromatosis, J. Comput. Assist Tomogr. 43 (1) (2019) 29–38.
[51] M. Braschi-Amirfarzan, et al., Role of imaging in management of desmoid-type fibromatosis: a primer for radiologists, Radiographics 36 (3) (2016) 767–782.
[52] T.K. Subhawong, et al., MRI volumetrics and image texture analysis in assessing systemic treatment response in extra-abdominal desmoid fibromatosis, Radio. Imaging Cancer 3 (4) (2021), e210016.
[53] J.J. Findeis-Hosey, K.Q. McMahon, S.K. Findeis, Von hippel-lindau disease, J. Pedia Genet 5 (2) (2016) 116–123.
[54] M.E. Aronow, et al., Von Hippel-Lindau disease: update on pathogenesis and systemic aspects, Retina 39 (12) (2019) 2243–2253.
[55] S.P. Rednam, et al., Von Hippel-Lindau and hereditary pheochromocytoma/paraganglioma syndromes: clinical features, genetics, and surveillance recommendations in childhood, Clin. Cancer Res. 23 (12) (2017) e68–e75.
[56] A.M. Vanbinst, et al., A focused 35-minute whole body MRI screening protocol for patients with von Hippel-Lindau disease, Hered. Cancer Clin. Pr. 17 (2019) 22.
[57] J. Shell, et al., The utility of (68)Gallium-DOTATATE PET/CT in the detection of von Hippel-Lindau disease associated tumors, Eur. J. Radio. 112 (2019) 130–135.
[58] M.X. Wang, et al., Tuberous sclerosis: current update, Radiographics 41 (7) (2021) 1992–2010.
[59] S.K. Goergen, M.C. Fahey, Prenatal MR imaging phenotype of fetuses with tuberous sclerosis: an institutional case series and literature review, AJNR Am. J. Neuroradiol. (2022).
[60] H.M. Hulshof, et al., Fetal brain magnetic resonance imaging findings predict neurodevelopment in children with tuberous sclerosis complex, J. Pedia 233 (2021) 156–162 e2.
[61] V.S. Katabathina, et al., Hereditary gastrointestinal cancer syndromes: role of imaging in screening, diagnosis, and management, Radiographics 39 (5) (2019) 1280–1301.
[62] V.S. Katabathina, C.O. Menias, S.R. Prasad, Imaging and screening of hereditary cancer syndromes, Radio. Clin. North Am. 55 (6) (2017) 1293–1309.
[63] H. Northrup, et al., Updated international tuberous sclerosis complex diagnostic criteria and surveillance and management recommendations, Pedia Neurol. 123 (2021) 50–66.
[64] C.E. Morin, et al., Thoracoabdominal imaging of tuberous sclerosis, Pedia Radio. 48 (9) (2018) 1307–1323.
[65] T. Frebourg, et al., Guidelines for the Li-Fraumeni and heritable TP53-related cancer syndromes, Eur. J. Hum. Genet 28 (10) (2020) 1379–1386.
[66] C.P. Kratz, et al., Cancer screening recommendations for individuals with Li-Fraumeni syndrome, Clin. Cancer Res. 23 (11) (2017) e38–e45.
[67] S.A. Anupindi, et al., Diagnostic performance of whole-body MRI as a tool for cancer screening in children with genetic cancer-predisposing conditions, AJR Am. J. Roentgenol. 205 (2) (2015) 400–408.
[68] A. Al-Salameh, et al., Clinical aspects of multiple endocrine neoplasia type 1, Nat. Rev. Endocrinol. 17 (4) (2021) 207–224.
[69] C. Daccord, et al., Birt-Hogg-Dube syndrome, Eur. Respir. Rev. 29 (2020) 157.
[70] S. Sundaram, A.D. Tasker, N.W. Morrell, Familial spontaneous pneumothorax and lung cysts due to a Folliculin exon 10 mutation, Eur. Respir. J. 33 (6) (2009) 1510–1512.
[71] F.H. Menko, et al., Birt-Hogg-Dube syndrome: diagnosis and management, Lancet Oncol. 10 (12) (2009), 1199-206.
[72] S. Gupta, et al., The ABCs of BHD: an in-depth review of Birt-Hogg-Dube syndrome, AJR Am. J. Roentgenol. 209 (6) (2017) 1291–1296.
[73] D.E. Benn, B.G. Robinson, R.J. Clifton-Bligh, 15 YEARS OF PARAGANGLIOMA: clinical manifestations of paraganglioma syndromes types 1-5, Endocr. Relat. Cancer 22 (4) (2015) T91–T103.
[74] N. Tufton, A. Sahdev, S.A. Akker, Radiological surveillance screening in asymptomatic succinate dehydrogenase mutation carriers, J. Endocr. Soc. 1 (7) (2017) 897–907.
[75] A.G. Jurik, Multiple hereditary exostoses and enchondromatosis, Best. Pr. Res. Clin. Rheuma 34 (3) (2020), 101505.
[76] L. Fei, C. Ngoh, D.E. Porter, Chondrosarcoma transformation in hereditary multiple exostoses: a systematic review and clinical and cost-effectiveness of a proposed screening model, J. Bone Oncol. 13 (2018) 114–122.